

Journal of Biomedical Optics

SPIEDigitalLibrary.org/jbo

Small-animal radionuclide luminescence imaging of thyroid and salivary glands with ^{99m}Tc -pertechnetate

Federico Boschi
Marco Pagliuzzi
Barbara Rossi
Maria Paola Cecchini
Giancarlo Gorgoni
Matteo Salgarello
Antonello E. Spinelli

Small-animal radionuclide luminescence imaging of thyroid and salivary glands with ^{99m}Tc -pertechnetate

Federico Boschi,^a Marco Pagliuzzi,^b Barbara Rossi,^c Maria Paola Cecchini,^a Giancarlo Gorgoni,^d Matteo Salgarello,^d and Antonello E. Spinelli^b

^aUniversity of Verona, Department of Neurological, Neuropsychological, Morphological and Motor Sciences, Strada Le Grazie 8, 37134 Verona, Italy

^bSan Raffaele Scientific Institute, Medical Physics Department and Centre for Experimental Imaging, Via Olgettina 60, Milan, Italy

^cUniversity of Verona, Department of Pathology and Diagnostics, Strada Le Grazie 8, 37134 Verona, Italy

^dOspedale Sacro Cuore Don Calabria, Nuclear Medicine Department, Via Sempredoni, 5-37024 Negrar (Verona), Italy

Abstract. The *in vitro* and *in vivo* detection of visible photons from radioisotopes using optical techniques is a fast-growing field in molecular imaging. ^{99m}Tc -pertechnetate is used as an alternative to ^{123}I in imaging of the thyroid and is generally imaged with gamma cameras or single photon emission tomography instruments. The uptake in the thyroid tissue is mediated by the sodium-iodide symporter (NIS), a glycoprotein that actively mediates iodide transport into the thyroid follicular cells and several extrathyroidal tissues. The luminescence of the gamma emitter ^{99m}Tc -pertechnetate in order to visualize its biodistribution in healthy small living animals by using a commercial optical imaging system is investigated. Here we show that in Nu/Nu mice, the uptake of ^{99m}Tc -pertechnetate in the thyroid gland and in salivary glands is very detectable by using radionuclide luminescence imaging. We also found light emission from the stomach in accordance with the literature. The localization of the light signals in the anatomical regions where the radiopharmaceutical is expected, confirmed by resections, shows that it is possible to image NIS-expressing tissues. © 2013 Society of Photo-Optical Instrumentation Engineers (SPIE) [DOI: 10.1117/1.JBO.18.7.076005]

Keywords: radioisotope luminescence imaging; ^{99m}Tc -pertechnetate; thyroid imaging; small animals.

Paper 130187R received Apr. 4, 2013; revised manuscript received May 20, 2013; accepted for publication May 21, 2013; published online Jul. 10, 2013.

1 Introduction

Radioisotope luminescence imaging (RLI) is a novel optical imaging technique based on the detection of visible photons generated by processes related to nuclear decays.¹

Within the RLI field, Cerenkov luminescence imaging (CLI) is a very fast-growing technique²⁻⁹ based on the detection of light generated when charged particles travel in a dielectric with a velocity greater than the speed of light in the medium itself. The energy threshold for Cerenkov radiation (CR) emission is dependent on the medium. For example, the threshold for a beta particle travelling in water is around 263 keV. CLI allows the detection of CR generated by both beta plus and beta minus emitters with an endpoint energy greater than the threshold.

Preclinical visualization of the thyroid gland using CR was investigated in mice by Jeong in 2011 (Ref. 10), and recently our group obtained the first Cerenkov image of a human thyroid of a patient treated with ^{131}I for hyperthyroidism.¹¹

As mentioned before, beta emitters with endpoint energy greater than the Cerenkov threshold are visible with CLI. However, despite the smaller light output, alpha and gamma emitters are also visible via RLI.

The imaging of alpha emitters was developed recently using ^{225}Ac (Ref. 12) and ^{241}Am (Ref. 13) and we demonstrated that the faint emission from biological tissues using alpha emitters is detectable with a conventional optical imager equipped with a charge-coupled device (CCD) camera.

In a preliminary work,¹⁴ we investigated the *in vivo* imaging of ^{99m}Tc -methylene-diphosphonate (^{99m}Tc -MDP) by using a small animal optical imaging system and covering the animal with a slab of bismuth germanate scintillating material. In a subsequent work,¹⁵ particular attention was focused on investigating the luminescence induced by ^{99m}Tc without any scintillating materials. More precisely, we measured the time decay of the optical signal in a vial containing ^{99m}Tc and we performed *in vivo* imaging using ^{99m}Tc -sestamibi and ^{99m}Tc -MPD.

In conventional nuclear medicine, ^{99m}Tc ($^{99m}\text{TcO}_4^-$) is commonly used as a substitute for ^{123}I for the imaging of thyroid.¹⁶ More precisely, the uptake of ^{99m}Tc -pertechnetate into the thyroid tissue is mediated by the sodium-iodide symporter (NIS), a transmembrane glycoprotein that actively mediates iodide (and other anions like TcO_4^-) transport into the thyroid follicular cells and several extrathyroidal tissues. Pertechnetate is thus used as an alternative medium for imaging of NIS-dependent functions, like transport of substrate into the thyroid gland and secretory function of the salivary glands and gastric mucosa.¹¹

The biodistribution of pertechnetate has been well characterized in the past showing that the principal NIS-bearing tissues are the thyroid, salivary glands, and the stomach.^{17,18}

Like $^{123}\text{I}^-$ and $^{131}\text{I}^-$, ^{99m}Tc -pertechnetate has a long and successful history of use in the diagnosis of thyroid cancer; moreover NIS expression has been found in more than 80% of human mammary cancers, and, thus, NIS has emerged as a potential target for radiotherapy of nonthyroid malignancies that express the endogenous or transfected symporter.¹⁷

This work can be considered a proof of principle; more precisely, the main goal of this paper is to show for the first time

Address all correspondence to: Federico Boschi, University of Verona, Department of Neurological, Neuropsychological, Morphological and Motor Sciences, Strada Le Grazie 8, 37134 Verona, Italy. Tel: +39 (0)45 802 7155; Fax: +39 (0)45 802 7163; E-mail: federico.boschi@univr.it

that using optical methods it is possible to image the parotid glands and the thyroid of a mouse injected with ^{99m}Tc -pertechnetate. In our opinion this result can be useful considering the large availability and the moderate costs of preclinical optical imaging devices with respect to small animals single photon emission tomography (SPECT) scanners.

2 Materials and Methods

2.1 RLI Acquisition

RLI images were acquired by using the Spectrum animal imaging system (Perkin-Elmer, Hopkinton, USA). The instrument is equipped with a cooled (-90°C) back-thinned, back-illuminated CCD camera.

The CCD has an active array of 1920×1920 pixels with a dimension of 13 microns. RLI data *in vivo* and *ex vivo* were obtained by acquiring images with the following parameters: exposure time = 300 s, $f = 1$, binning $B = 16$, without emission filter.

The dynamic RLI data were acquired every 5 min. Light radiance measurements were done on regions of interest manually drawn over the animal's neck; the luminescence signals are expressed as photons per seconds per squared centimeter per steradian ($\text{p/s/cm}^2/\text{sr}$).

Images were acquired and analyzed with Living Image 4.2 (Perkin-Elmer) and were corrected for the dark measurements.

2.2 Animal Handling

A total of six nude mice of 25 ± 5 g were injected in the tail vein with about 70 MBq/0.2 mL of 0.9% NaCl of ^{99m}Tc -pertechnetate. Nude mice were used in order to allow the detection of a small number of optical photons.

Mice were placed in a supine position 15 min before the imaging session in order to reduce the persistent luminescence that is responsible for the background noise in the case of luminescence images.¹⁹

During images acquisition, the mice were kept under gaseous anesthesia (2% of isoflurane and 1 l/min of oxygen). In order to optimize and image the thyroid uptake,¹⁸ three animals were sacrificed 35 min after injection and the salivary glands were removed.

Three animals were imaged continuously for 70 min, mainly to investigate *in vivo* the salivary glands' uptake.¹⁸

The specificity of RLI thyroid and salivary glands imaging with ^{99m}Tc -pertechnetate was investigated using a control mouse injected in the tail vein with 75 MBq/0.15 mL of ^{99m}Tc -MDP. This tracer is known to be not thyroid specific, binding mainly to the bony structures of the animal.

All the animal handling was approved by the Institutional Ethical Committee according to the regulations of the Italian Ministry of Health and the European Communities Council (86/609/EEC) directives.

3 Results

In this section, we present the results obtained from the *in vivo* and *ex vivo* experiments described in Sec. 2.

Figure 1 shows an RLI image of two animals 35 min after injection of ^{99m}Tc -pertechnetate. As one can see by looking at the image, both mice reveal light emission from anatomical regions corresponding to the salivary glands, thyroid, and stomach-intestine.

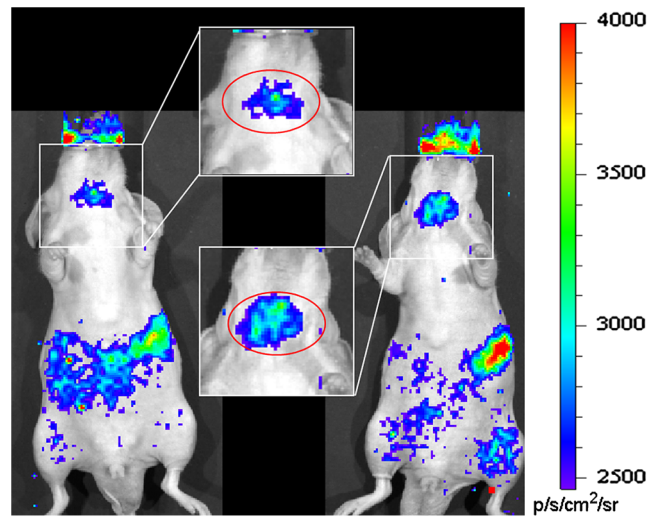


Fig. 1 RLI image of the ^{99m}Tc -pertechnetate distribution in Nu/Nu mice placed in supine position. The zoomed regions corresponding to salivary-thyroid gland and along with the stomach-intestine are the most important sources of light emission.

As shown by the time activity curve in Fig. 2, RLI dynamic imaging reveals a monotonic uptake of the radiopharmaceutical in the salivary glands-thyroid with respect to a background region.

In this case, the signal to background ratio of the salivary glands region measured after 70 min from the tracer injection was found to be equal to 1.85.

These results prove that the ^{99m}Tc -pertechnetate accumulated in the salivary glands anatomical district is visible with RLI and detectable over the background emission.

Thirty-five minutes after ^{99m}Tc -pertechnetate injection, three animals were sacrificed and the skin removed in order to visualize the thyroid and salivary glands. More precisely, with the aim of separating the signal contribution of the salivary glands with respect to the signal from the thyroid, the salivary glands were extracted from the body and imaged separately.

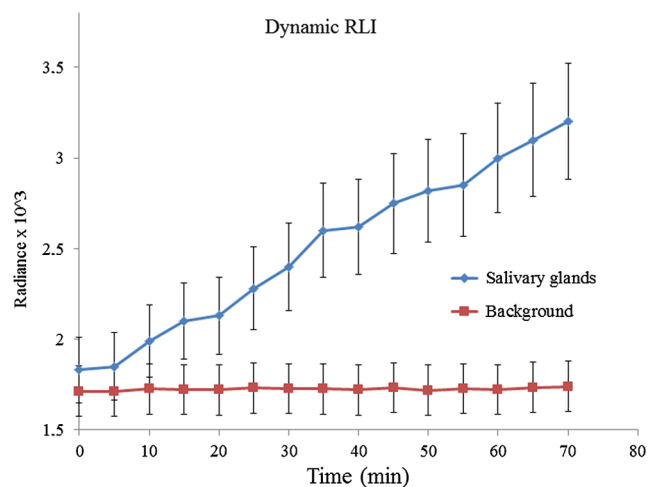


Fig. 2 Average radiance ($\text{p/s/cm}^2/\text{sr}$) measured on ROIs corresponding to the salivary glands-thyroid and a background region. Dynamic data were acquired for 70 min after ^{99m}Tc -pertechnetate injection. The measured radiance was obtained from a single mouse and the error bars correspond to the standard deviation of the radiance within the ROI.

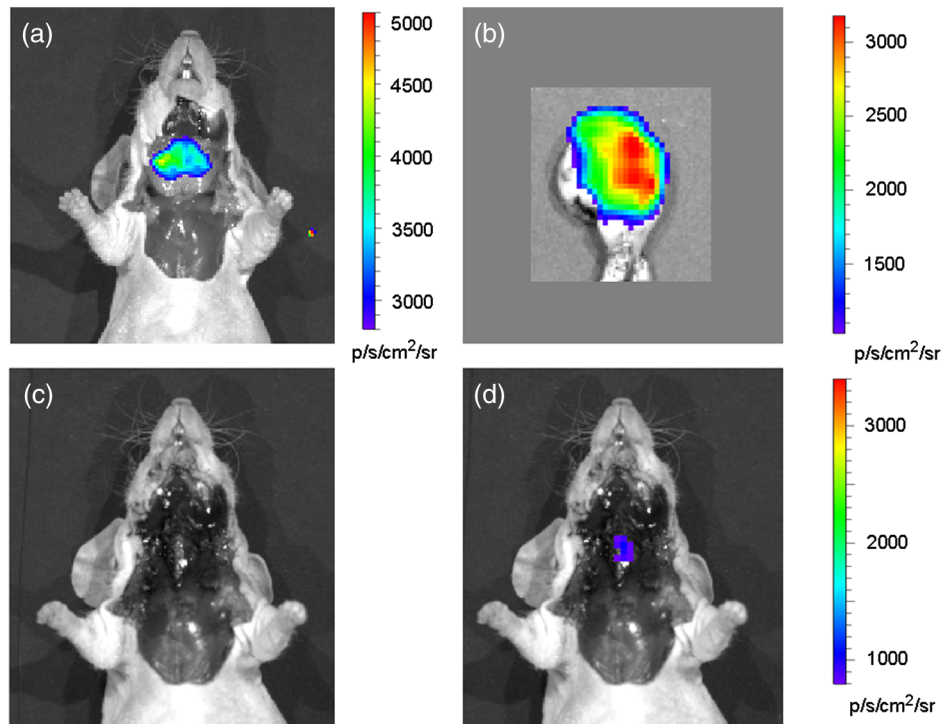


Fig. 3 The panel (a) shows an RLI image of the ^{99m}Tc -pertechnetate distribution in the salivary glands *in situ*; the emission of the extracted salivary glands is presented in panel (b). Panel (d) shows the emission from the thyroid gland *in situ* with respect to the anatomical image (photograph) presented in panel (c).

Luminescence images were acquired as reported in Fig. 3(a). The image shows the light signal coming from the salivary glands complex *in situ*. The most relevant signal comes from the upper part of the glands in the rostro-caudal direction.

Figure 3(b) shows the light emission from the salivary glands alone, and in order to visualize the contribution of the very small murine thyroid gland, the mice were imaged again after the extraction of the salivary glands. Figure 3(d) shows the emission coming from the thyroid gland *in situ*; the localization of the

light source is well in accordance with the corresponding anatomical position as shown in Fig. 3(c).

The total flux escaping from the thyroid gland is about one order of magnitude less than the flux escaping from the salivary glands.

Figure 4 shows an RLI of a control mouse injected in the tail vein with 75 MBq/0.15 mL of ^{99m}Tc -MDP. As expected, no specific salivary-thyroid binding of the tracer can be found.

4 Discussions and Conclusions

In this work, we showed the first evidence of detectability of ^{99m}Tc -pertechnetate using an optical imaging technique in living mice. The luminescence signal in the salivary and the thyroid glands were also measured *ex vivo*.

The RLI dynamic data shown in Sec. 3 are in accordance with the results obtained using conventional nuclear medicine imaging with a gamma camera.^{17,18}

We found that the total flux escaping from the thyroid gland is one order of magnitude less than the flux escaping from the salivary glands. Moreover, the thyroid gland is located deeper inside the tissue when the animals are in a supine position, so it is possible to argue that the contribution of the signal escaping from the living animals is due mainly to the salivary glands uptake.

We would like to underline here that with the term salivary glands we are referring to the submandibular-sublingual complex (SSC), which is composed of the submandibular and sublingual glands located in the ventral cervical region. The submandibular gland is almond-shaped and the sublingual gland lens-shaped, lying lateral to the rostral third of the submandibular gland. The two glands are separated by a thin sheet of connective tissue and the excretory ducts emerge rostrally from both glands.²⁰ The submandibular gland is mainly

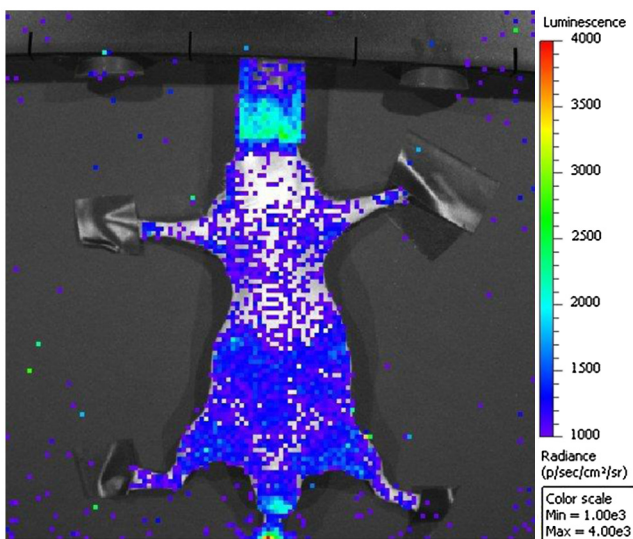


Fig. 4 RLI of a control mouse injected in the tail vein with 75 MBq/0.15 mL of ^{99m}Tc -MDP; the image shows no specific salivary-thyroid binding of the tracer.

composed of serous cells and the sublingual gland is mainly composed of mucous cells. The nonhomogeneity of light signal detected in the salivary glands could suggest different uptakes of ^{99m}Tc -pertechnetate in the glands themselves and could reflect different functionalities of the two components of the SSC, but this hypothesis needs to be further investigated.

Results obtained using a control mouse injected with ^{99m}Tc -MDP showed, as predicted, no specific salivary-thyroid binding with respect to ^{99m}Tc -pertechnetate.

In conclusion, the luminescence images presented in this work reveal that ^{99m}Tc -pertechnetate uptake in NIS-expressing cells were well visualized using a commercial optical imager instrument, and, thus, RLI with ^{99m}Tc -pertechnetate has potential applications for salivary glands and thyroid gland research in small animals. This result suggests that ^{99m}Tc -pertechnetate could be used in the future to image NIS-bearing cancer cells that can be found in 80% of human mammary cancers.

Acknowledgments

The authors would like to acknowledge the Cariverona Foundation for financial support.

References

1. A. E. Spinelli et al., "Optical imaging using radioisotopes: a novel multimodal approach to molecular imaging," *Q. J. Nucl. Med. Mol. Imag.* **56**(3), 279–289 (2012).
2. R. Robertson et al., "Optical imaging of Cerenkov light generation from positron-emitting radiotracers," *Phys. Med. Biol.* **54**(16), N355–N365 (2009).
3. A. E. Spinelli et al., "Cerenkov radiation allows in vivo optical imaging of positron emitting radiotracers," *Phys. Med. Biol.* **55**(2), 483–495 (2010).
4. F. Boschi et al., "In vivo (18)F-FDG tumour uptake measurements in small animals using Cerenkov radiation," *Eur. J. Nucl. Med.* **38**(1), 120–127 (2011).
5. A. E. Spinelli et al., "Cerenkov radiation imaging of beta emitters: in vitro and in vivo results," *Nucl. Instrum. Meth. A* **648**(Suppl 1), S310–S312 (2011).
6. A. E. Spinelli et al., "Multispectral Cerenkov luminescence tomography for small animal optical imaging," *Opt. Express* **19**(13), 12605–12618 (2011).
7. A. E. Spinelli and F. Boschi, "Unsupervised analysis of small animal dynamic Cerenkov luminescence imaging" *J. Biomed. Opt.* **16**(12), 120507 (2011).
8. F. Boschi et al., "Quantum dots excitation using pure beta minus radioisotopes emitting Cerenkov radiation," *RSC Advances* **2**(29), 11049–11052 (2012).
9. A. E. Spinelli and F. Boschi, "Optimizing in vivo small animal Cerenkov luminescence imaging," *J. Biomed. Opt.* **17**(4), 040506 (2012).
10. S. Y. Jeong et al., "Combined Cerenkov luminescence and nuclear imaging of radioiodine in the thyroid gland and thyroid cancer cells expressing sodium iodide symporter: initial feasibility study," *Endocr. J.* **58**(7), 575–583 (2011).
11. A. E. Spinelli et al., "First human Cerenkography," *J. Biomed. Opt.* **18**(2), 020502 (2013).
12. A. Ruggiero et al., "Cerenkov luminescence imaging of medical isotopes," *J. Nucl. Med.* **51**(7), 1123–1130 (2010).
13. F. Boschi et al., "Optical imaging of alpha emitters: simulations, phantom, and in vivo results," *J. Biomed. Opt.* **16**(12), 126011 (2011).
14. F. Boschi et al., "Combined optical and single photon emission imaging: preliminary results," *Phys. Med. Biol.* **54**(23), L57–L62 (2009).
15. A. E. Spinelli et al., "Optical imaging of Tc-99m based tracers, in vitro and in vivo results," *J. Biomed. Opt.* **16**(11), 116023 (2011).
16. U. Y. Ryo et al., "Thyroid imaging agents: a comparison of I-123 and Tc-99m pertechnetate," *Radiology* **148**(3), 819–822 (1983).
17. L. S. Zuckier et al., "Kinetics of perrhenate uptake and comparative biodistribution of perrhenate, pertechnetate, and iodide by NaI symporter-expressing tissues in vivo," *J. Nucl. Med.* **45**(3), 500–507 (2004).
18. P. R. Franken et al., "Distribution and dynamics of ^{99m}Tc -pertechnetate uptake in the thyroid and other organs assessed by single-photon emission computed tomography in living mice," *Thyroid* **20**(5), 519–526 (2010).
19. F. Boschi et al., "Spontaneous luminescence background in living Nu/Nu mice," *Adv. Mol. Imaging* **2**(2), 5–11 (2012).
20. A. Sbarbati et al., "Magnetic resonance imaging of the submandibular-sublingual complex," *Acta Anatomica* **149**(1), 63–69 (1994).